FINAL REPORT

A Design Tool for Robust Composite Structures

Frank Zok

Materials Department
University of California, Santa Barbara
Santa Barbara, CA 93106

Norman Fleck, Vikram Deshpande

Cambridge University Engineering Department
Trumpington Street, Cambridge CB2 1PZ
United Kingdom.

June 2010

REPORT DOCUMENTATION PAGE

Form Approved
OMB No. 0704-0188

1. REPORT DATE *(DD-MM-YYYY)*	2. REPORT TYPE	3. DATES COVERED *(From - To)*
12-06-2010	Final Technical Report	01/30/2009-09/29/2009

4. TITLE AND SUBTITLE
A Design Tool for Robust Composite Structure

5a. CONTRACT NUMBER

5b. GRANT NUMBER
HR0011-09-1-0011

5c. PROGRAM ELEMENT NUMBER

6. AUTHOR(S)
Zok, Francis; Fleck, Norman; Deshpande, Vikram

5d. PROJECT NUMBER

5e. TASK NUMBER

5f. WORK UNIT NUMBER

7. PERFORMING ORGANIZATION NAME(S) AND ADDRESS(ES)
The University of California, Santa Barbara
Santa Barbara, CA 93106

8. PERFORMING ORGANIZATION REPORT NUMBER

9. SPONSORING/MONITORING AGENCY NAME(S) AND ADDRESS(ES)
DARPA
3701 North Fairfax Drive
Arlington, VA 22203-1714

10. SPONSOR/MONITOR'S ACRONYM(S)
DARPA

11. SPONSORING/MONITORING AGENCY REPORT NUMBER

12. DISTRIBUTION AVAILABILITY STATEMENT
Approved for Public Release; Distribution is Unlimited

13. SUPPLEMENTARY NOTES

14. ABSTRACT
New opportunities exist for enhancing the impact resistance of organic matrix composites while simultaneously imparting multifunctionality. They draw upon the existence of organic fibers, especially Dyneema®. The principal objectives of the present study were to ascertain the fundamental mechanical properties of Dyneema® fibers and assess strategies for integrating these fibers into load-bearing structures. The results reveal that the tensile strength of Dyneema® composites increases by a factor of 2 and the ductility by almost a factor of 3 over the strain rate range 10-3 s-1 to 104 s-1. One consequence is that the Dyneema® composites outperform by a wide margin (factor of 4) the ballistic resistance of CFRP composites at the same areal density. Moreover, it has been demonstrated that Dyneema® composites can be integrated into metallic sandwich panels with either metallic prismatic cores or polymer foam cores using mechanical attachment schemes. When integrated into such structures, the full impact resistance of the composites is realized only when the backside is unconstrained at the impact site and is thus free to deform. Dyneema® fibers can also be incorporated into hybrid carbon fiber composites as through-thickness reinforcements, with benefits in impact resistance and retained compressive strength.

15. SUBJECT TERMS
Dyneema® fibers; sandwich panels; hybrid fiber composites; impact and ballistic resistance

16. SECURITY CLASSIFICATION OF:	17. LIMITATION OF ABSTRACT	18. NUMBER OF PAGES	19a. NAME OF RESPONSIBLE PERSON
			Frank Zok

INSTRUCTIONS FOR COMPLETING SF 298

a. REPORT	b. ABSTRACT	c. THIS PAGE			19b. TELEPONE NUMBER (*Include area code)*
U	U	U	SRA	22	805-893-8699

1. Background

Since their inception, organic matrix composites (OMCs) have lacked robustness when loaded dynamically. This deficiency has limited implementation despite their compelling weight advantages. The most prevalent problems are as follows. (i) Subsurface delaminations develop upon local impact, degrading the in-plane compressive strength. Such delaminations are difficult to detect and characterize, with adverse consequences for assured load capacity following an impact event. Impact by foreign objects (so-called foreign object damage: FOD) occurs for a wide range of configurations in applications ranging from airframes to fans to military vehicles. Airframes are susceptible to delaminations caused by mishandling during maintenance and upon impact during flight. (ii) Vehicles are subject to impulsive loads caused by blasts as well as impact by fragments and projectiles. Such dynamic loads induce multiple mechanisms of damage: including delamination, fiber failure and tearing. (iii) Composite fans used for aero-turbines are susceptible to impact by soft objects (bird strike) that, beyond a threshold kinetic energy (KE), can cause either delamination or gross failure. Moreover, containment of that fan, once failed, by a woven composite hybrid represents a new arena for substantial weight reduction.

It has been appreciated for some time that delaminations can be suppressed by one of two methods. (I) A relatively small area fraction of transverse fibers, normal to the loading plane, can substantially impede the extension of incipient delaminations, by imposing tractions as they extend and open. The mechanics governing these so-called "bridging" effects is sufficiently well-established that the benefits of transverse fibers can be predicted. Heretofore, the challenge has been in the implementation. Conventional methods of introducing transverse fibers damage the in-plane fibers, resulting in diminished tensile and compressive strengths that obviate the weight benefits of the composite. (II) Adhesive bonding of thin Ti alloys onto the surface of a composite can diminish the momentum transmitted into the composite when impacted by a high KE soft object. Plastic deformation of the alloy reduces the amplitude of the elastic waves that extend into the composite. When appropriately configured, the stresses remain below the delamination threshold, even in the absence of transverse fibers. However, delamination between the metal and composite upon dynamic loading presents implementation problems.

2. The New Opportunities

New opportunities exist to bring into being robust solutions to these impact limitations. They draw upon the existence of organic fibers, especially Dyneema®, having exceptional specific stiffness and strain to failure. (a) One manifestation arises in the context of composites produced using these fibers in 0/90 laminate form, which provide remarkable ballistic protection for vehicles and aircraft as well as for personnel (body armor). The mechanisms that allow these composites to perform successfully have yet to be elucidated. (b) Another manifestation entails their use in 3-D woven hybrids, greatly enhancing the complexity of configurations that can be manufactured. Because of their flexibility and high failure strain, Dyneema® fibers are used for the transverse reinforcements, while glass or C fibers are retained for their in-plane benefits, without degradation.

3. Objectives

The principal objectives of the present study are four-fold:

(i) To ascertain the fundamental mechanical properties of Dyneema® composites over a wide range of strain rates relevant to ballistic and blast loadings. This requires design and implementation of new tensile test methods to overcome the challenges in gripping these composites.

(ii) To employ the tensile test results in calibrating a constitutive model for Dyneema® laminates and assess the predictive capability of the model in the context of both ballistic and blast performance. A related goal is to compare the blast response of Dyneema® laminates with that of a carbon fiber reinforced polymer (CFRP) composite.

(iii) To identify and assess strategies that allow implementation of Dyneema® composites into multifunctional sandwich structures constructed from metallic alloys.

(iv) To investigate the potential performance benefits derived from the addition of Dyneema® fibers in 3D orthogonal weaves with carbon fibers employed for the warp and weft yarns and Dyneema® for the z-yarns.

The matrix of materials probed is summarized in Table I.

In a broader context, a related goal of this program is the further development of an Integrated Computational Materials Engineering (ICME) capability, with a focus on force protection systems. A vision for ICME is outlined in the ensuing recommendations.

Table I: Material, Test and Characterization Matrix

Composite Material	C-Fiber Laminate	Woven C-Fiber	Dyneema Fiber Laminate	3-D Woven Hybrid PMC
Metallic Constituents	Ti-6Al-4V Back/ Front Faces			
	304 Stainless Steel Back/Front Faces			
Test Methods	Ballistic Tests with Spheres/Cylinders			
	Drop Weight Tests			
	Compressive Strength After Impact Open Hole Tensile and Compressive Strengths			
Characterization	X-ray Tomography/ Delamination Fiber Fragmentation			

3. Ballistic Performance of Dyneema® Composites

3.1 Basic Tensile Measurements. Baseline mechanical measurements were performed on the composites to establish their reference properties. Such tests are substantially more challenging than on C and glass fiber reinforced composites, because of the low slip resistance of the fibers, manifest as extreme fiber pull-out from the matrix. To achieve successful tests, a large grip region with small gage section was required (Figure 1(a)). Tests in this configuration were performed on both cross-ply (0°/90°) and unidirectional (0°) composites. High strain rate tests were performed using a specially developed dynamic test rig, shown in Figures 1(b) and (c). A Dyneema® tow was adhered to an aluminium block and the block was impacted by a projectile, to impose a high strain rate in the range of $300 - 10^4\ s^{-1}$.

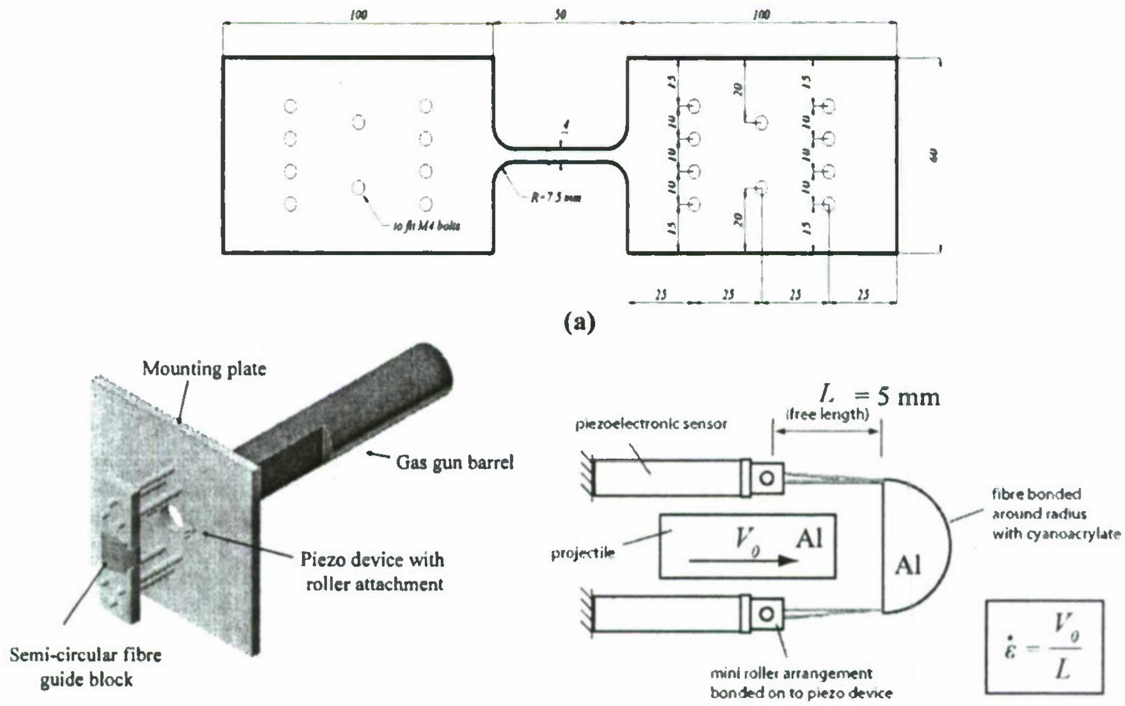

(b) (c)

Figure 1: (a) The configuration and gripping arrangement used to measure the tensile properties of Dyneema® fiber composites at low strain rates. (b. c) Dynamic test rig used for performing high strain rate tensile tests in a gas gun.

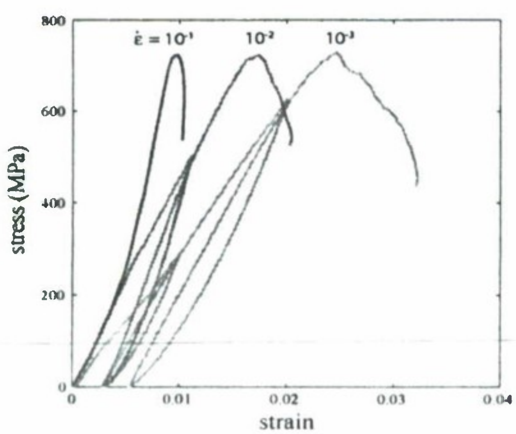

Figure 2: Representative tensile test results on the 0°/90° composite at low strain rates.

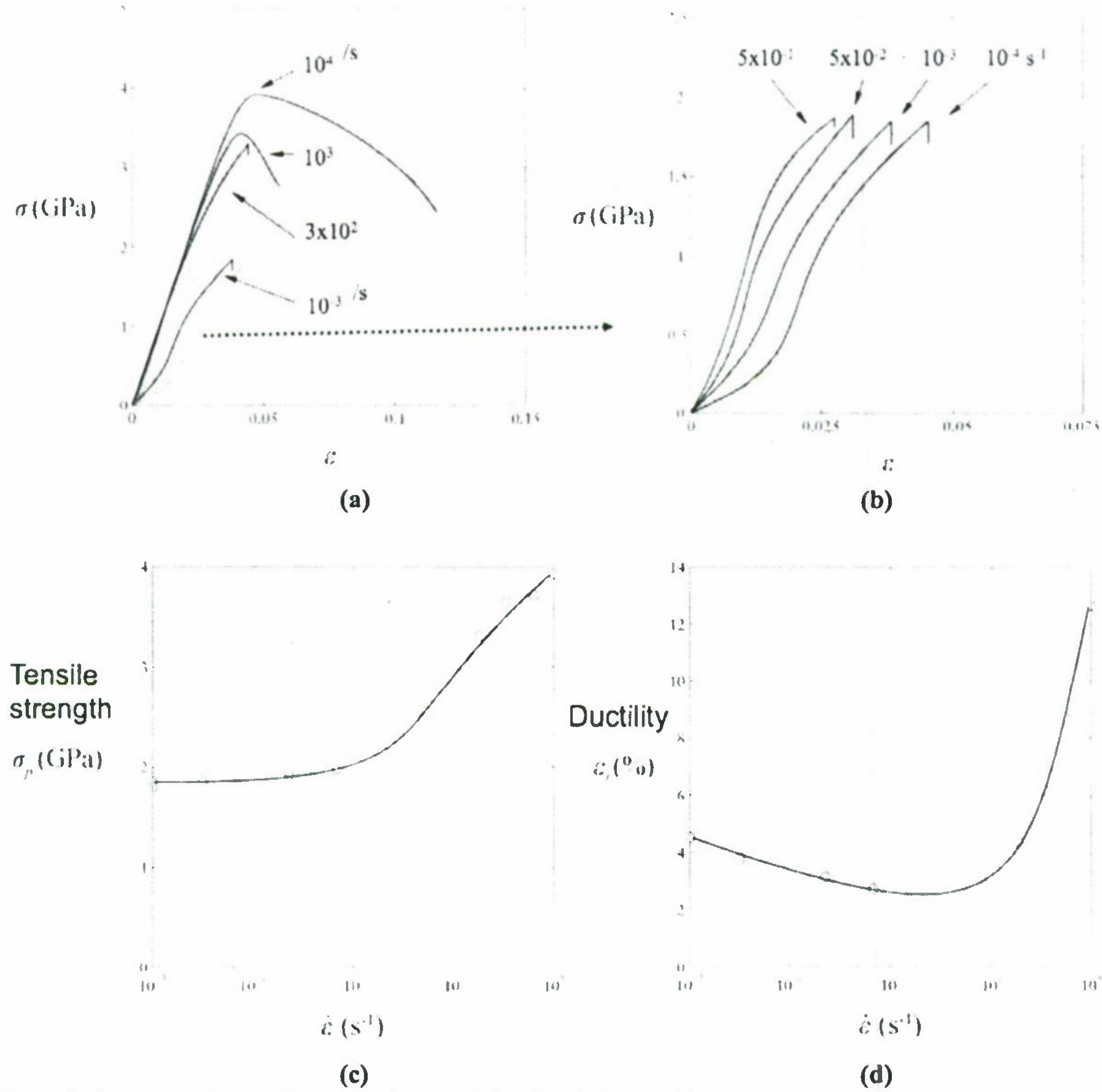

Figure 3: Representative tensile test results on unidirectional ribbon with 83 volume % fibers.

The tests reveal that the 0°/90° composite tensile strength exhibits no strain-rate sensitivity up to strain rates of 0.1 s^{-1}. However, within this range, the modulus increases rapidly with increasing strain rate. Accordingly, the strain at failure decreases as the strain rate increases. Similar trends are obtained on the unidirectional ribbon in the same strain rate domain. However, at yet higher strain rates, the strength increases by a factor of 2 and the ductility increases by a factor of 3, giving an overall increase in energy absorption per unit volume of a factor of 6. It remains a future challenge to determine the mechanism of this strain rate sensitivity.

3.2 Ballistic Performance. Ballistic tests were conducted in a gas gun facility on three different materials, all with the same areal density: 304 stainless-steel, a 0/90 woven C composite and a 0/90 Dyneema® composite. The tests were performed with steel spheres, 13 mm in diameter.

The objective was to measure the maximum velocity that plates of these materials could sustain before the projectile penetrates. Circular plates, 100mm in diameter, were used, gripped rigidly around the perimeter using bolts. The tests were monitored with a high-speed camera to determine the onset of penetration as well as the deformation modes of the plates. The ballistic results are summarized on Figure 4. Images of the impact events are presented on Figure 5. The remarkable outcome is that the Dyneema® composite has a ballistic limit *four times larger than that for the C-fiber reinforced composite.* While several hypotheses have been proposed to explain this performance advantage, none have yet been rigorously tested and analyzed.

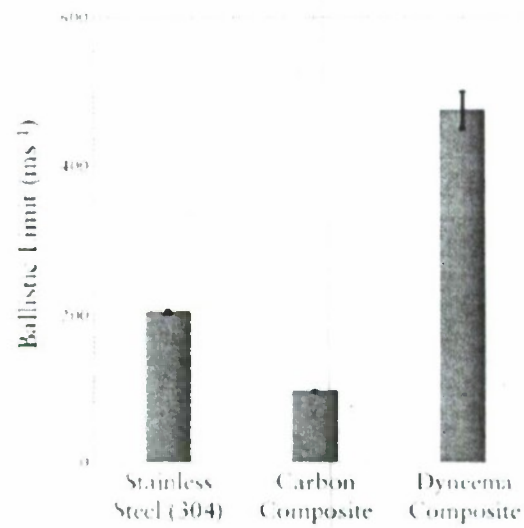

Figure 4: A comparison of the ballistic limits for the hree materials impacted by steel spheres.

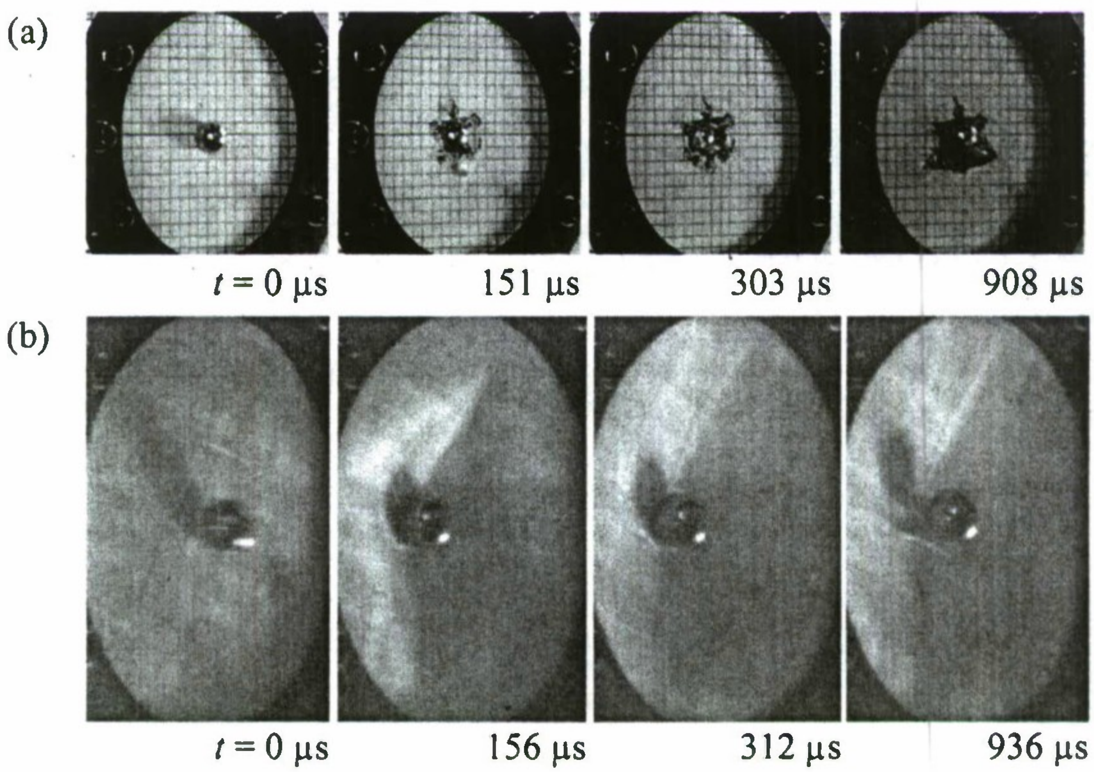

Figure 5: Impact of steel ball with (a) CFRP plate at 95 m/s and (b) Dyneema® plate at 350 m/s. The images show the deformation of the impacted face.

3.3. Hybrid Systems and Multi-hit Response. The multihit characteristics of C-fiber composite panels has been assessed by bonding stainless steel plates to the composite and measuring its ballistic performance after exposing the same location to two consecutive impacts. The results are presented as a cross plot of the ballistic performance after the first and second impacts. A synopsis is presented on Figure 6. For these tests the ballistic limit subject to a single impact was 120m/s. After an initial impact just below this limit, the panels survived all second impacts up to 100m/s. Namely, only within a small corner of the response diagram was there any significant degradation after the first impact. The hybrid system is thus much more resistant to multiple impacts than either C-composites or steel plates separately. These results suggest an aggressive research agenda on the benefits of metal/composite hybrids for their resistance to multiple hit degradation.

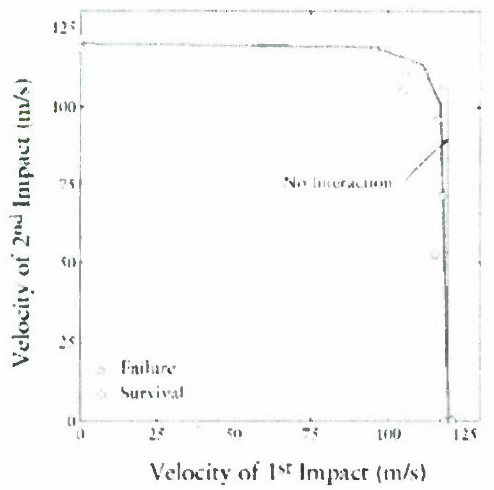

Figure 6: A response diagram for a stainless steel/C-fiber composite hybrid subject to multiple impacts. A small interaction effect among impacts is only evident in the top right corner.

4. Blast Performance

4.1 Dyneema® Plates vs. CFRP Sandwich Panels. Under blast loading conditions, metallic sandwich panels are capable of outperforming monolithic plates at the same mass/area for two primary reasons. (i) A fluid/structure interaction effect at the front face reduces the momentum imparted to the panel. (ii) The sandwich panel can be designed to behave in a soft manner when subjected to impulsive loading. This softness reduces the pressure exerted on the back face and thereby diminishes both the deflections and the reaction forces at the supports. Beneficial results have been demonstrated for several core configurations, including the square honeycomb and the X-core. Moreover, it has been demonstrated that the latter effect can be reproduced at laboratory scale by impacting with Al-foam projectiles that impart impulsive loads comparable in amplitude and duration to those imposed by a blast wave.

Consequently, to assess whether similar benefits are possible with composites, C-fiber reinforced sandwich panels with square honeycomb cores have been fabricated (Figure 7(a)) and tested using Al-foam projectiles that impart pressures of order 100 MPa for a duration about 0.1 ms. Similar tests have been made on monolithic composite plates having the same mass/area. The metric for initial assessment has been the maximum displacement experienced by the back face, ascertained using high-speed camera measurements.

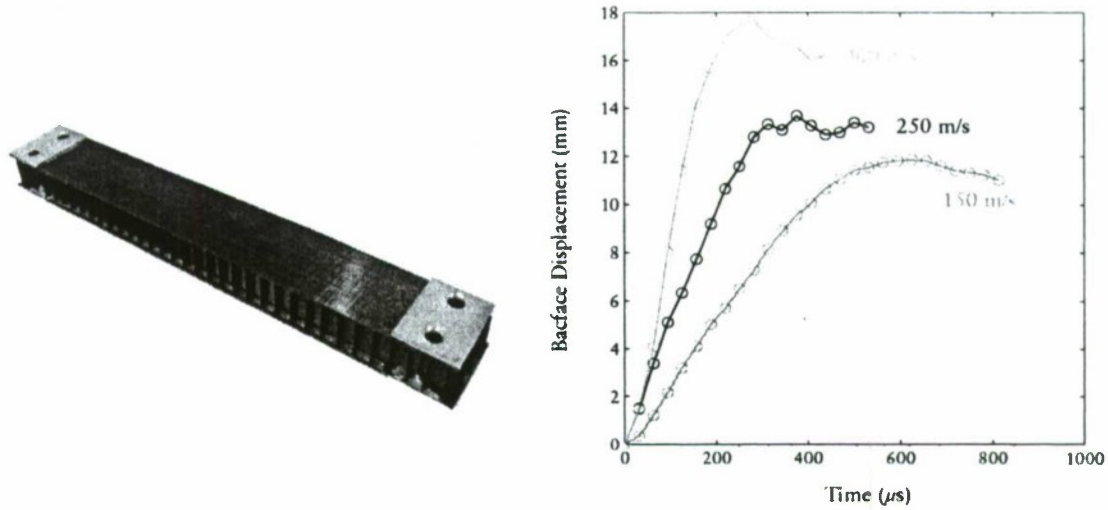

(a) **(b)**

Figure 7: (a) A CFRP sandwich panel with square honeycomb core and (b) back face deflection measurements made at several impact velocities.

A synopsis of the measurements is presented on Figure 8. Whereas the sandwich panels exhibit smaller deflections at the lower impulse levels, they offer no benefit at high impulse. Moreover, the maximum impulse that can be sustained without failure due to fiber rupture is essentially the same for the monolith and the sandwich beams. The sandwich and monolithic measurements have been replicated using finite element simulations with the composites treated using the Hashin-Rotem model (Figure 9). Both the core and face materials were built up from a series of plies with bonding between the core and the face sheets modeled using a cohesive approach. Delamination between the plies was also modeled via a cohesive framework. The material parameters in the model (such as the tensile/compressive strength of the laminates) were measured using separate materials tests. This relatively simple modeling approach predicts the measurements to an acceptable level of accuracy.

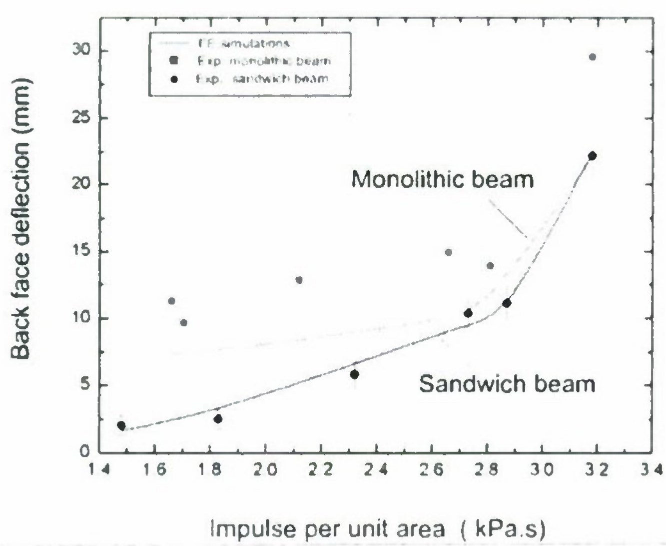

Given the minimal benefit of the sandwich configuration, no further effort was devoted to CFRP sandwich panels within this project.

Figure 8: Measurements of the back face deflections of sandwich and monolithic beams impacted by Al foam projectiles over a range of impulse levels. Also shown are the results of the finite element simulations.

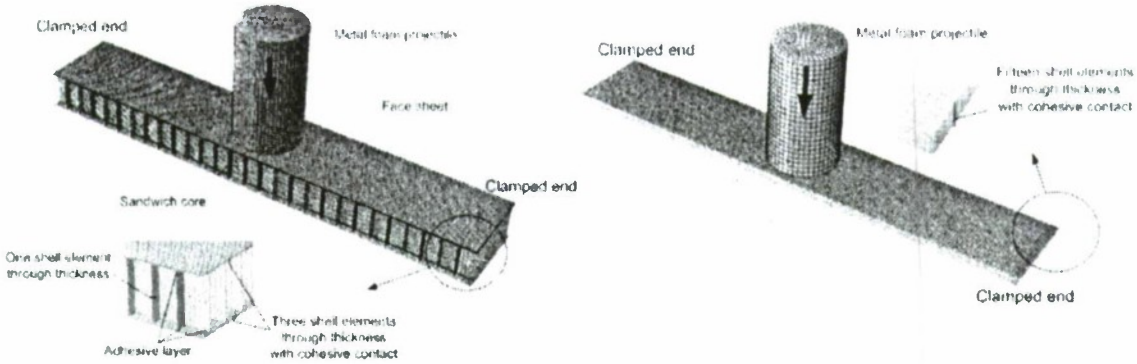

Figure 9: The finite element meshes used for the simulations presented on Figure 8.

4.2 Role of Matrix in Blast Performance. In order to probe the (potential) role of the weak matrix in the Dyneema® composites, it is instructive to compare the blast response of the Dyneema® beams with that of a 0/90 IM7/8552 CFRP in both the uncured and cured state. This was accomplished using metal foam projectiles to simulate blast loading. The projectiles (diameter of 28.5mm and length of 50mm) were fired from a gas gun at a velocity in the range of 100-600 ms^{-1}. The ABAQUS Explicit finite element (FE) model of the test is shown in Figure 10. The FE analysis made use of the aforementioned constitutive law for Dyneema® and a metal foam constitutive law for the projectile. The FE analysis reveals that failure occurs from the bolt holes, and the predictions are conservative as the FE model assumes the low strain-rate response of the fibers (Figure 11). The uncured CFRP has a low shear strength and is comparable in performance to the Dyneema® (Figure 12). In contrast, the cured CFRP has a large stress concentration at the supports and fails prematurely.

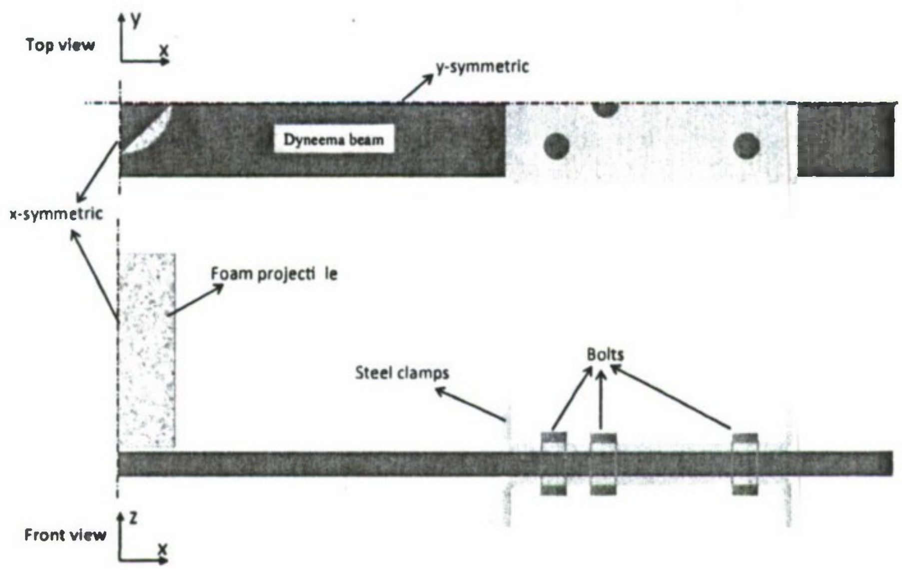

Figure 10: Finite element model of a Dyneema® beam impacted by a metal foam projectile.

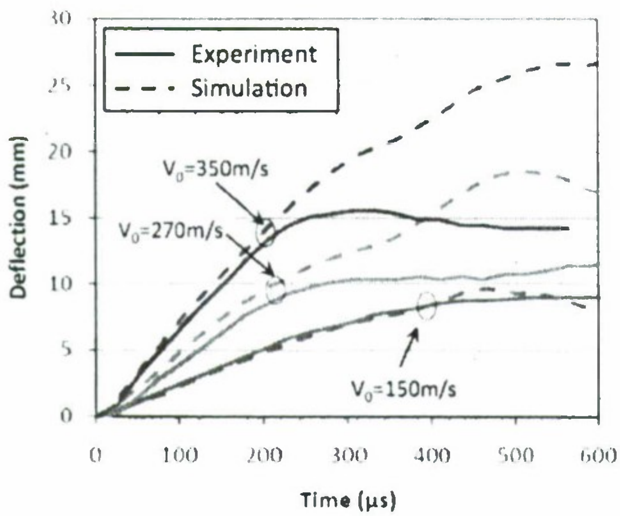

Figure 11: Comparisons of measured and computed deflections.

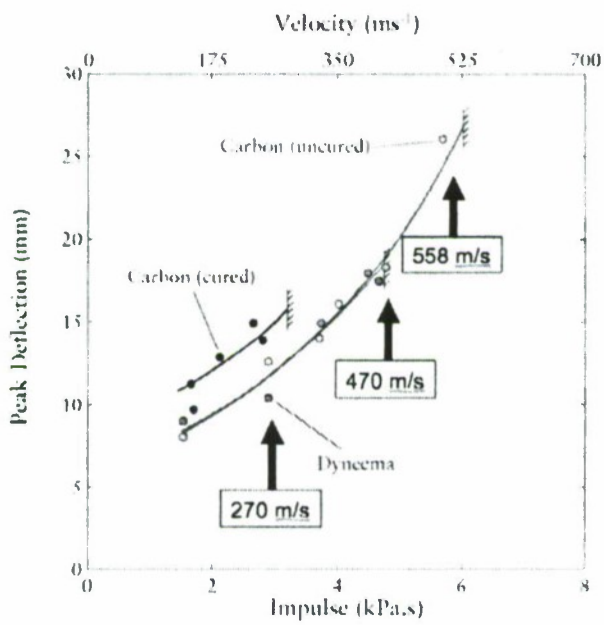

Figure 12: The relative blast performance of Dyneema® and 0/90 CFRP panels of equal areal density.

5. Integration of Dyneema® Composites into Metallic Sandwich Structures

The preceding results demonstrate that Dyneema® composites exhibit substantially higher ballistic limits relative to CFRP composites. Nevertheless, their potential for use in structural applications (beyond those that require solely ballistic resistance) is severely limited by their extreme mechanical anisotropy. For instance, the ±45° tensile strength of a cross-ply laminate is a mere 1% of that obtained in the 0°/90° orientation. The through-thickness strength is lower yet. The implication is that simple metal/Dyneema® laminates will not have the requisite out-of-plane strength to satisfy structural requirements. One goal of the present activity was to identify and assess strategies that allow implementation of these composites into multifunctional structures constructed from metallic alloys.

A preliminary assessment has been made of the impact resistance of 2D laminates comprising Dyneema® plates with face sheets of a high-strength Ti alloy (notably Ti-6Al-4V). Three configurations with equivalent areal density have been probed. They are distinguished by the thicknesses t_f and t_b of the front and back Ti face sheets, characterized by the non-dimensional parameter:

$$\Omega = \frac{(t_f - t_b)}{(t_f + t_b)}$$

The two limiting cases are those in which all of the Ti resides either in the back face ($\Omega = -1$) or the front face ($\Omega = 1$). To ensure equal areal densities, the thickness of the Dyneema® plate was held constant (3.1 mm) whereas the face sheet thicknesses were required to be in the domain defined by $t_f + t_b = 3.04$ mm. The sheets were bonded to one another using a room-temperature curing organic adhesive. Ballistic tests were performed in a gas gun using 7.6 mm diameter hardened steel spheres with impact velocity of 500±20 m/s.

Effects of Ω on ballistic performance are summarized in Figures 13 and 14. For $\Omega = -1$, penetration of the structure by the projectile occurs with highly localized deformation of either the Dyneema® or the Ti sheets. The exit velocity is about half that upon impact. Penetration also occurs for $\Omega = 0$, although it is accompanied by more extensive deformation around the impact site and with reduced exit velocity. In the limiting case of $\Omega = 1$, *penetration does not occur.* The associated deformation within the Dyneema® is extensive, progressing to the clamped boundaries, accompanied by delamination over the entire Dyneema/Ti interfacial area.

The results suggest that the full impact resistance of the Dyneema® is realized only when its back side is unconstrained at the impact site and is thus free to deform. The importance of this constraint was illustrated through an additional experiment for which $\Omega = -1$ but (in contrast to the preceding experiments) with a 10 mm space placed between the two sheets (Figure 12(d)). Under these conditions, the Dyneema® undergoes extensive deformation (up to the point where it makes contact with the Ti), decelerating the projectile sufficiently so as to prevent penetration through the Ti.

The implications of these experiments are two-fold. (i) For successful implementation of Dyneema® into metallic structures, the Dyneema® layers must remain largely unconstrained on their back side. (ii) The design must ensure that out-of-plane strength is not dictated by that of the Dyneema. This precludes use of 2D laminates that rely exclusively on adhesives for bonding.

Based on these insights, two candidate structural designs, illustrated in Figure 15, have been devised and tested. Both are sandwich configurations with high structural efficiency (both stiffness and strength), yet without significant constraint on bending and stretching of the Dyneema. The designs also ensure that the sandwich response is not limited by the transverse strength of the Dyneema. Assembly has been accomplished using adhesives and mechanical attachments. In one manifestation (Figure 15(a)), the Dyneema® composite is embedded into a corrugated metal core sandwich, between the core and the outer face sheet. A complementary design (Figure 15(b)) builds on the same basic principles but with the corrugated metal core replaced by a lightweight polymeric foam. One challenge is to identify a core material with the appropriate combination of elastic-plastic properties: that is, strong enough to impart structural integrity yet soft enough to allow extensive deformation of the Dyneema® without significant impediment.

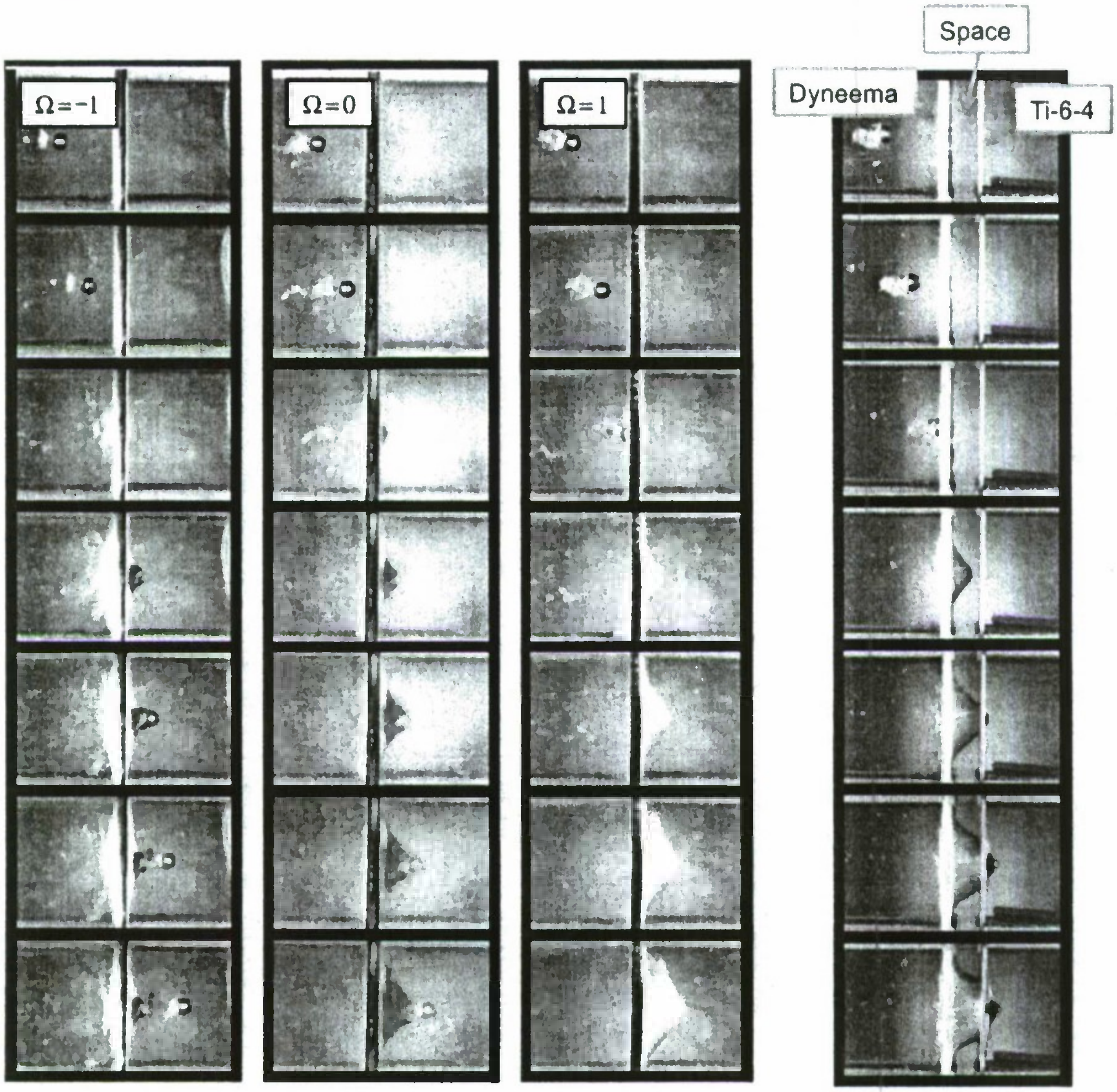

(a) (b) (c) (d)

Figure 13: (a-c) Optical images of ballistic impact tests obtained with a high speed camera, showing effects of Ω. (d) Analogous experiments showing the beneficial effect of a space between the Dyneema® and the Ti for the case Ω=-1. Here the projectile did not penetrate through the Ti face sheet. (In all cases the interframe time is 25 μs.)

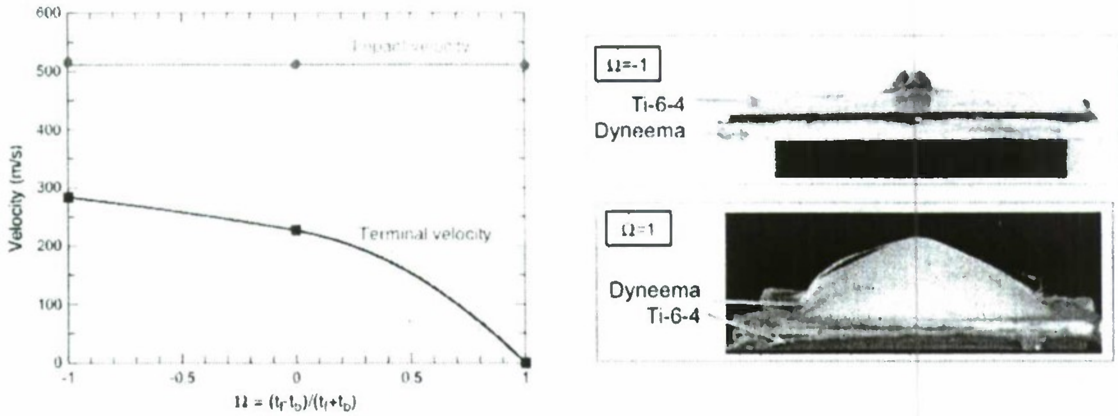

(a) (b)

Figure 14: (a) Effects of Ω on exit projectile velocity. (b) Macrophotographs of specimens at the two extreme values of Ω.

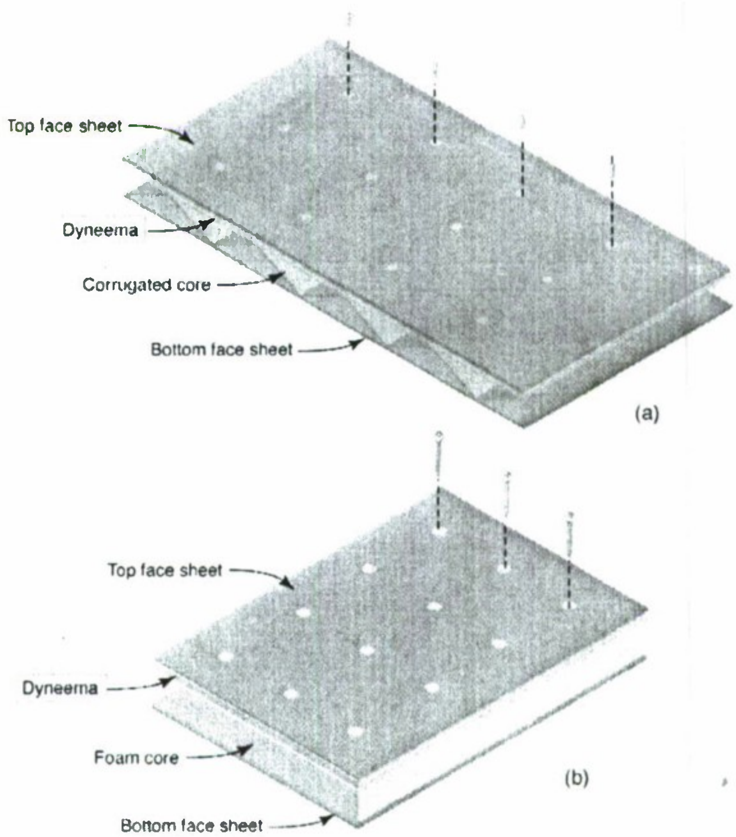

Figure 15: Conceptual designs that integrate Dyneema® into multi-material sandwich structures.

Preliminary assessments have been made on sandwiches with 304 stainless steel face sheets (Figure 16). One set had 304 stainless steel corrugated cores and the other Divinycell PVC foam with low relative density (5%). For comparison, sandwich panels without Dyneema® were also fabricated and tested. The panels were subjected to impact tests using 7.6 mm diameter steel spheres at velocities in the range 200–800 m/s. In situ observations of the impact process were made using a high speed Imacon framing camera. The key results are presented in Figures 17-19.

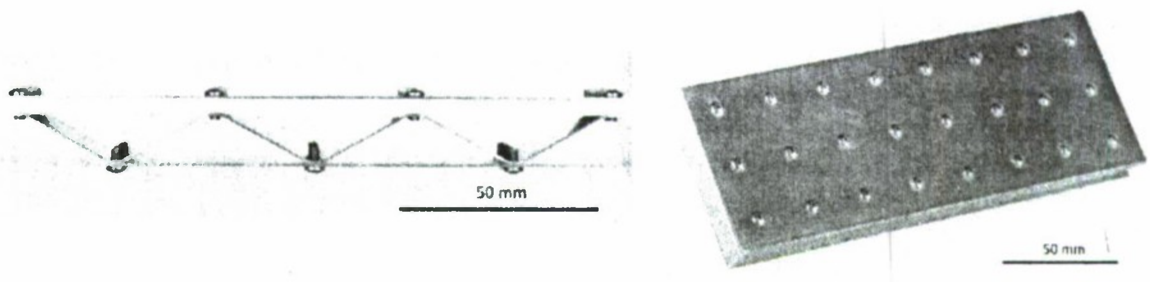

(a) (b)

Figure 16: Sandwich panels with embedded Dyneema® composite layers: (a) corrugated core, (b) Divinycell foam core. All metallic parts are made of 304 stainless steel.

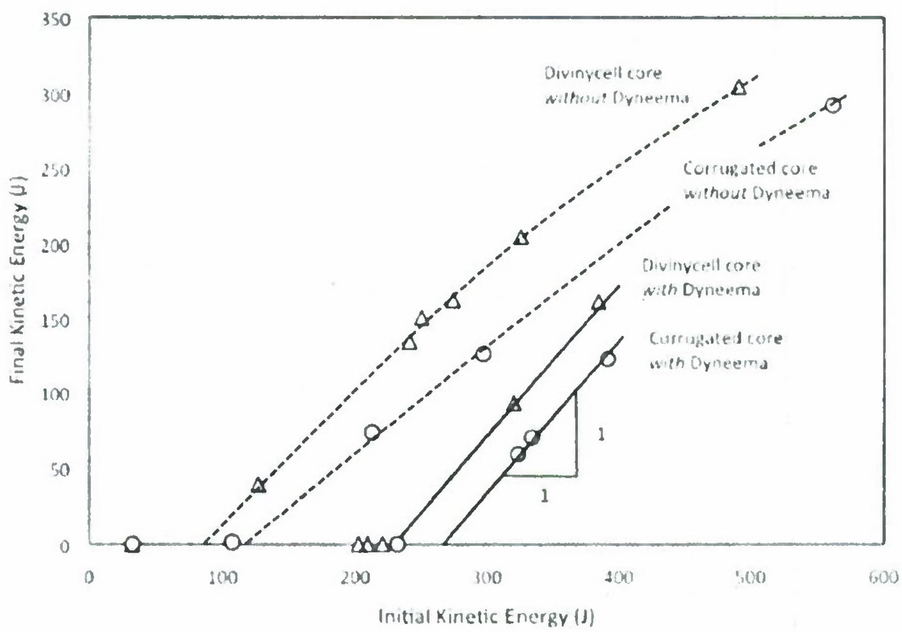

Figure 17: Ballistic performance of corrugated and foam core sandwiches both with and without Dyneema® composite layers.

The ballistic limit of the corrugated core panel with Dyneema® is slightly greater than that of the panel with the foam core. In both systems, beyond the ballistic limit, the loss in kinetic energy during the penetration process is essentially constant. That is, the rate of change of terminal kinetic energy with initial kinetic energy is unity. The ballistic limits of the panels without Dyneema® are significantly lower, with the corrugated core system again exhibiting slightly better performance than with the foam core. Furthermore, the differences in ballistic limits due to the presence of the Dyneema® are the same in both systems. This is manifested in a constant shift in the kinetic energy at the ballistic limit (about 150 J). The inference is that the Dyneema®

composite is equally effective in both the corrugated core and the foam core. Evidently, the foam core is sufficiently soft to allow the Dyneema® to bend and stretch as it would otherwise (in the absence of a backing material).

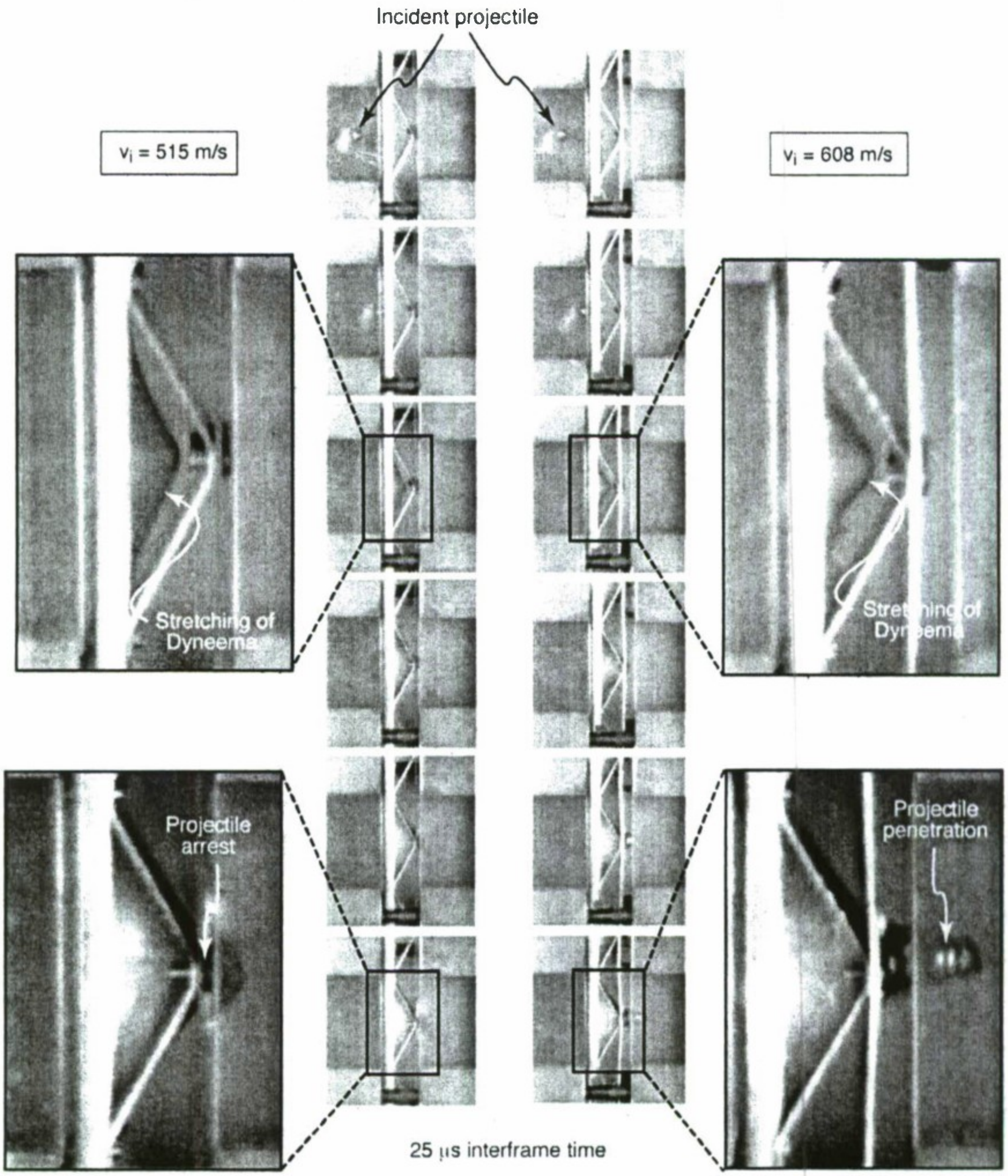

Figure 18: Optical images of ballistic impact tests on corrugated core panels with embedded Dyneema® composite layer, slightly below (left) and slightly above (right) the ballistic limit. Insets show the bending and stretching of Dyneema® during impact.

The in-situ observations on the corrugated panels (Figure 18) reveal the spatial extent of stretching of the Dyneema® layers. At or below the ballistic limit, the deformation extends to the nodal attachment points: a distance of about 25 mm on either side of the impact site. Although similar features are evident above the ballistic limit, the lateral growth of the stretched volume occurs somewhat more slowly, because of increasing inertial effects. Thus, the expectation is that the efficacy of the Dyneema® in ballistic performance may decrease at yet higher velocities.

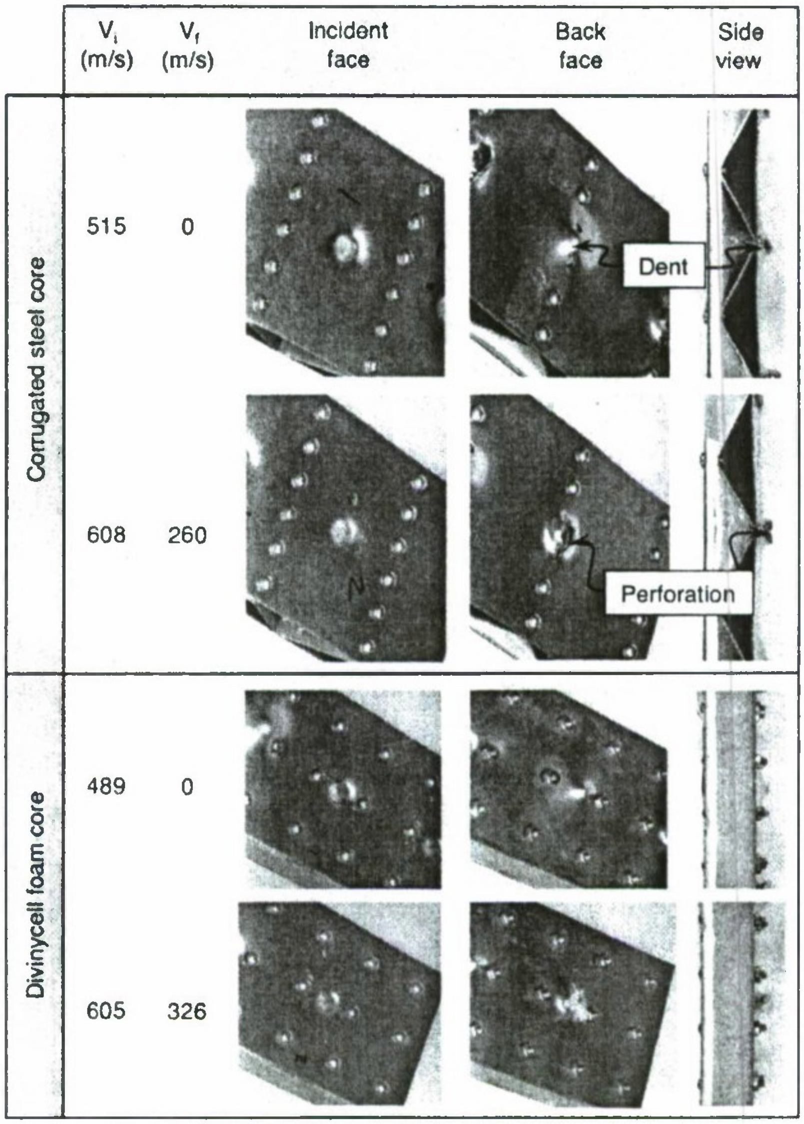

Figure 19: Photographs of representative tested sandwich panels with embedded Dyneema® composite layers, both below and above the ballistic limit.

6. Hybrid Dyneema®/Carbon Fiber Reinforced Polymer Matrix Composites

6.1 Motivation. The principal objective of this part of the study was to investigate the potential performance benefits derived from the addition of Dyneema® fibers to carbon fiber reinforced polymer (CFRP) composites. The study focuses specifically on 3D orthogonal weaves with carbon employed for the warp and weft yarns and Dyneema® ® for the z-yarns. Experiments on a series of composite panels with various volume fractions of z-yarns demonstrate that the pristine and retained in-plane compressive strength following impact is indeed enhanced by the presence of the z-yarns. The benefits derive from a reduced propensity for delamination during impact and buckling of the in-plane fibers during subsequent compressive loading. Analogous trends are obtained for open-hole compression.

6.2. Experimental Details. Three sets of composite panels with various volume fractions of z-yarns were fabricated by 3TEX using vacuum assisted resin transfer molding (VARTM). The processing route started with fabrication of 3D orthogonal weaves (Figure 20) with carbon employed for the warp and weft yarns and Dyneema® for the z-yarns. All warp layers were made of Toho Tenax HTS 40F13 fibers (800 tex, 12 ends/inch). The fill layers were made of Toho Tenax HTS 40 E13 fibers (400 tex, 10 ends/inch). Table 1 summarizes the specifications of the fabrics. The woven preforms were impregnated with West System 105 Epoxy Resin® mixed with a West System 206 Slow Hardener at a 5:1 ratio by vacuum-assisted resin transfer molding.

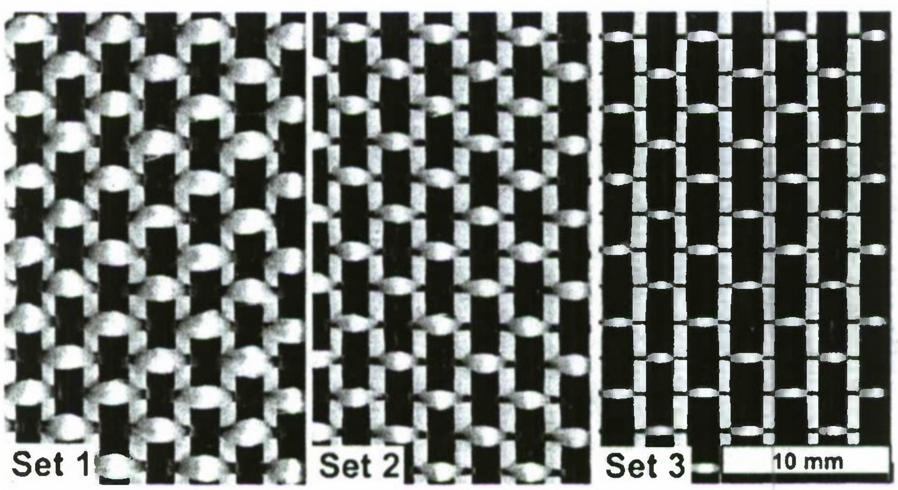

Figure 20: Optical images of the 3D fiber performs with carbon fibers employed for the warp and weft yarns (black) and Dyneema® for the z-yarns (white).

The compressive strength of the pristine samples was measured using a combined loading compression test fixture according to ASTM standard D6641. The test specimens were untabbed rectangular strips, 12 mm in width and 140 mm in length, prepared by water jet machining. Six specimens per set were tested at room temperature.

Table I: Weave specifications.

Specifications	Set 1	Set 2	Set 3
Number of warp layers	3	3	3
Number of weft layers	4	4	4
Z yarn	Dyneema® 1760	Dyneema® 880	Dyneema® 110
Fabric thickness	3.47 mm	3.06 mm	2.60 mm
Volume content of warp fibers	41.1%	44.2%	47.0%
Volume content of weft fibers	45.7%	49.1%	52.2%
Volume content of Z fibers (Dyneema®)	**13.2%**	**6.7%**	**0.8%**
Total fiber volume fraction in composite (estimated, from a geometric model)	52.3%	54.5	56.6

Flat, rectangular composite plates, 150 mm long and 100 mm wide, were subjected to an out-of-plane, concentrated impact event using a drop-weight device with a hemispherical impactor. The potential energy of the drop-weight, as defined by the mass and drop height of the impactor, was specified prior to test. Four plates per set were impacted at 25 J and 50 J. The residual compressive strength of the aforementioned impacted panels and open-hole panels were measured according to ASTM standard D7137. The test fixture utilizes flat, rectangular plates, 150 mm long and 100 mm wide. The top and the bottom of the test specimens are not clamped but are constrained from out of plane displacement or rotation. The side supports are knife edges, which provide no rotational constraint. The tests were performed using a hydraulic testing machine (MTS 810, Minneapolis, MN) at room temperature at displacement rate of 0.2 mm/s.

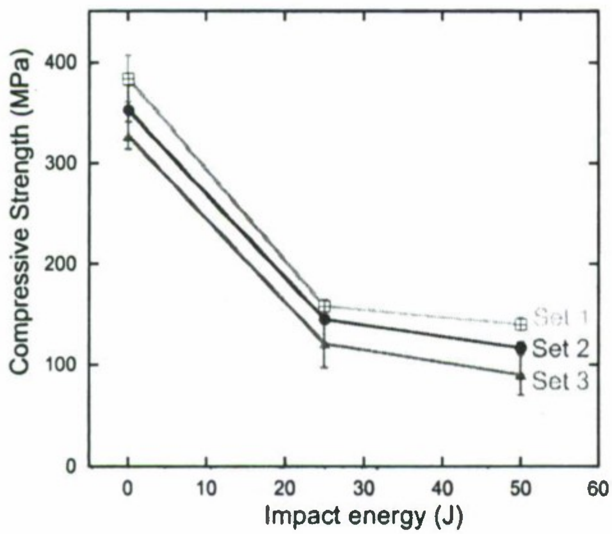

Figure 21: Effects of impact on retained compressive strength of the hybrid 3D composites.

6.3 Compressive Properties. Figure 21 shows the compressive strength values of the pristine samples and the residual compressive strength of impacted specimens as a function of impact energy. The results affirm that the compressive strength of the pristine samples as well as the retained in-plane compressive strength of the panels following impact is enhanced by the presence of the z-yarns, being highest in Set 1. These benefits derive from a reduced propensity for delamination during impact (Figure 22) and buckling of the in-plane fibers during subsequent compressive loading. Increasing the volume fraction of the z-yarns yields an apparent improvement. Similar trends are obtained in the compression strength of specimens with open holes (Figure 23).

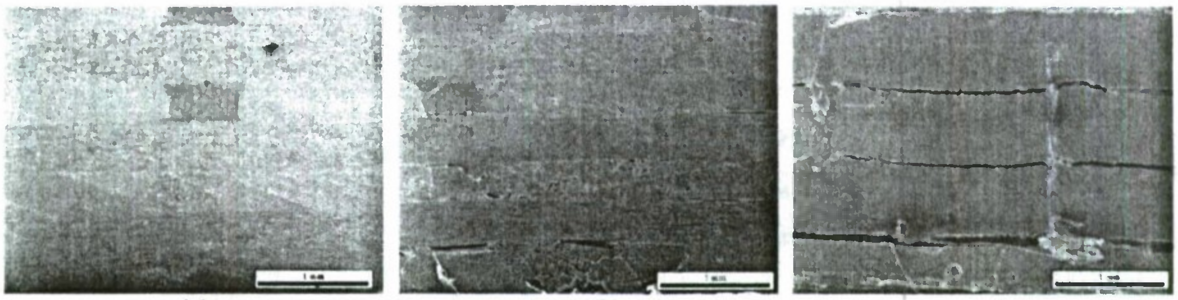

(a) (b) (c)

Figure 22: Scanning electron micrographs of cross-sections after 50 J impact: (a) Set 1, (b) Set 2, (c) Set 3.

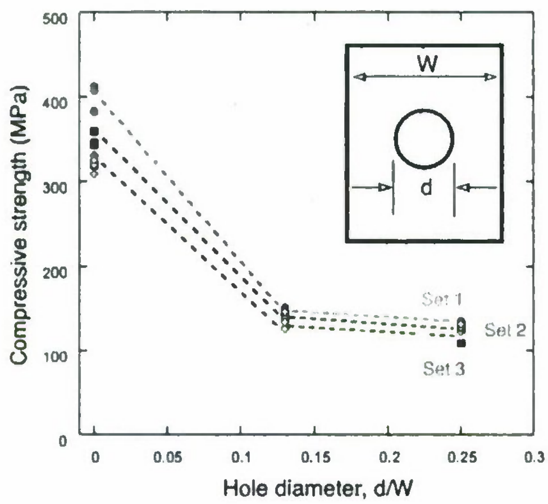

Figure 23: Effects of open holes on compressive strength. Panel width W=100 mm.

7. Conclusions

The key conclusions from this study follow:

(i) The tensile properties of Dyneema® composites exhibit a strong strain rate sensitivity. The strength increases by a factor of 2 and the ductility by almost a factor of 3 over the range 10^{-3} s^{-1} to 10^{4} s^{-1}.

(ii) The Dyneema® composites outperform by a wide margin (factor of 4) the ballistic resistance of CFRP composites at the same areal density. They also outperform CFRPs under blast-simulating loadings. These performance differences are attributable to the high strength and ductility of Dyneema® at high strain rates as well as the very weak matrix of the Dyneema® composites.

(iii) When integrated into metallic structures for force protection systems, the full impact resistance of these composites is realized only when the back side is unconstrained at the impact site and is thus free to deform. The spatial extent over which the composite is unconstrained is thus expected to play a crucial role in its ballistic performance.

(iv) Dyneema® composites can be integrated into metallic sandwich panels with either metallic prismatic cores, e.g. corrugated sheet, or polymer foam cores using mechanical attachment schemes. The benefits include high bending stiffness and strength along with enhanced penetration resistance.

(v) Dyneema® fibers can be incorporated into hybrid carbon fiber composites as through-thickness reinforcements. The principal benefit is in mitigating the delamination that occurs under impact loading and the associated reduction in the retained compressive strength.

It remains to exploit the various mechanisms and concepts identified in this study for the design of lightweight, multifunction systems with optimized ballistic and blast resistance.

8. Recommendations

Specific Outstanding Issues: The origins of the superior ballistic performance of the Dyneema® composites relative to other organic matrix composites and the implications for design of future force protection systems remain to be fully understood. Undoubtedly their exceptional strength and ductility are paramount. Yet some of the observed features cannot be rationalized on the basis of these properties alone. It has been proposed that the anisotropy in wave speeds plays an important role. Specifically, the high axial modulus of the fibers in combination with their low density (<1 g/cm^3) yields a high longitudinal wave speed (of order 10^4 m/s). In contrast, because of the low radial fiber modulus and the low modulus of the matrix, the wave speeds in the through thickness direction are 1–2 orders of magnitude lower. The strong anisotropy is expected to have important consequences for stress wave interactions in systems in which ceramics are in contact with Dyneema® composites. Specifically, when waves pass from the ceramic to the composite, the magnitudes of the reflected and transmitted waves as well as their subsequent propagation within the composite will be governed by both the large acoustic impedance mismatch as well as the wave speed anisotropy. Rapid wave spreading in the plane of the fibers is expected to increase the volume of material participating in the subsequent deformation and dissipation mechanisms and thus enhance the ballistic resistance. The low yield strengths of the matrices typically used with Dyneema® along with the intrinsically weak interfaces formed with these fibers are also expected to play a role in the dissipation of stress waves. Further progress in understanding the pertinent mechanics and mechanisms is expected to lead to the development of the principles underlying materials selection and design for enhanced ballistic and blast resistance. This will require further experimental investigations, e.g. of shock/stress wave propagation through composites and multi-layered systems, as well as the associated computational tools.

Long-Range Vision: In a broader context, the goal of accelerating the development of defense-critical platforms will be most effectively and rapidly achieved through structured programs that embody Integrated Computational Materials Engineering (ICME). ICME involves the integration of materials information, captured in computational material models and property databases, with product performance analysis and simulation of manufacturing processes (Figure 24(a)). ICME provides outstanding opportunities for significant economic benefits as well as enhanced national security. It will require coordination of the principal stakeholders – namely government agencies, industry, universities and professional organizations – in establishing a new infrastructure for education and research (Figure 24(b)). In light of the benefits of ICME to national security, the DOD should expand its leadership role in establishing a long-range coordinated ICME program. This will include identifying and pursuing key foundational engineering problems that will not only accelerate the materials/product development cycle in the near term but also enable the necessary ICME infrastructure to support long-term objectives.

A specific set of challenges needed to develop the ICME of force protection systems is illustrated in Figure 25.

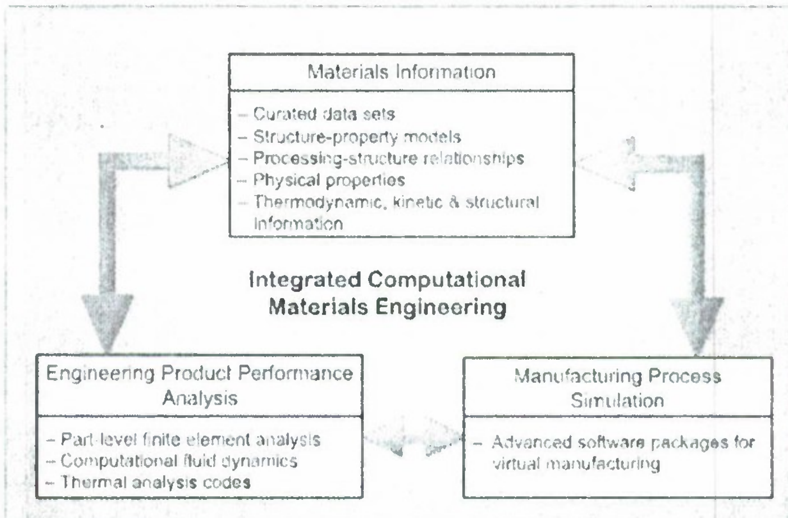

(a)

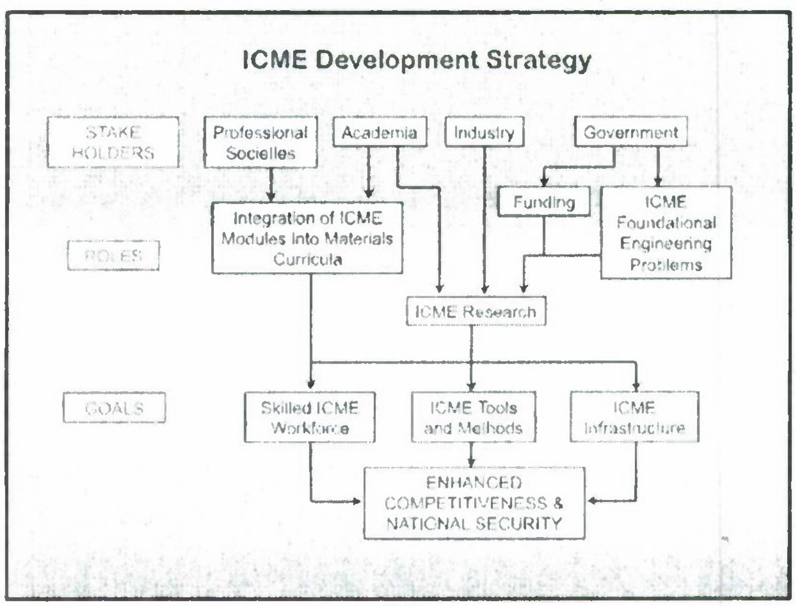

(b)

Figure 24: (a) The basic elements of Integrated Computational Materials Engineering. (b) The ICME development strategy. Adapted from "Integrated Computational Materials Engineering: A Transformational Discipline for Improved Competitiveness and National Security", Report of the National Materials Advisory Board, National Research Council of the National Academies, 2008 (http://www.nap.edu/catalog/12199.html)

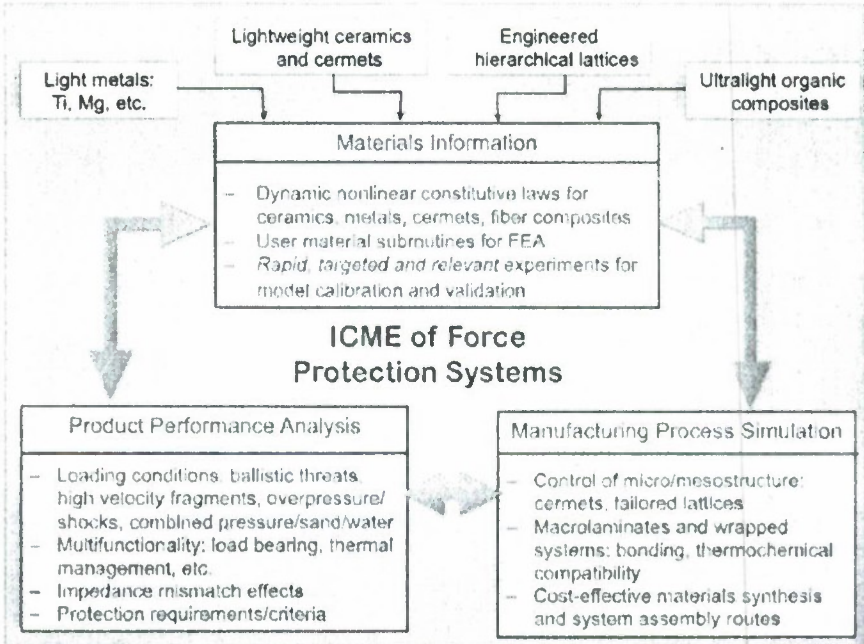

Figure 25: Proposed elements of an Integrated Computational Materials Engineering activity focused on force protection systems.

Acknowledgements: The authors greatly acknowledge the financial support of DARPA as well as the provision of Dyneema® fibers and composites from DSM.